Electronic Supplementary Material (ESI) for Materials Horizons.

Supporting Information for Molecular Design of DBA-type Five-membered Heterocyclic Rings to Achieve 200% Exciton Utilization for Electroluminescence

Qi Sun[⊥1], Yishi Wu[⊥4], Yuanyuan Cui[3], Can Gao[5], Qi Ou[1], Deping Hu[1], Lu Wang[1], Yue Wang[3], Huanli Dong[5], Jianzhang Zhao[6], Chunfeng Zhang[7], Zhigang Shuai*[1], Hongbing Fu[4], Qian Peng*[2,5]

[1]*MOE Key Laboratory of Organic Optoelectronics and Molecular Engineering, Department of Chemistry, Tsinghua University, Beijing, 100084, P. R. China*
E-mail: zgshuai@tsinghua.edu.cn

[2]*School of Chemical Sciences, University of Chinese Academy of Sciences, Beijing, 100049, P. R. China*
E-mail: qianpeng@ucas.ac.cn

[3]*College of Chemistry, Jilin University, Changchun 130012, P. R. China*

[4]*Department of Chemistry, Capital Normal University, Beijing 100048, P. R. China*

[5]*Institute of chemistry, Chinese Academy of Sciences, Beijing, 100049, P. R. China*

[6]*School of Chemical Engineering, Dalian University of Technology, 2 Ling Gong Road, Dalian 116024, P. R. China*

[7]*School of Physics, Nanjing University, Nanjing, 210093, China*
[⊥] These authors contributed equally to this work.

Experimental Procedures

1. Computational Methods

Firstly, we performed high level calculations using OpenMolcas package[1] to calculate the excitation energies of the six five-membered rings at the T_1 geometry in Scheme 1. Considering accuracy and the cost of calculation, we chose SA4-CASSCF (10,10) to optimized the T_1-geometry and MS4-CASPT2 (10,10) to complete the excitation energies, all with the cc-pVTZ basis set. TDDFT with Tamm-Dancoff approximation (TDA) can improve the accuracy of the calculated energy of triplet excited states.[2] Brédas et al. have been used these methods to successfully calculated ΔE_{ST} and $E(S_1)$ of some typical TADF molecules.[3] We use the same method to calculate the pyrazoline derivatives. The ground state and excited state geometries were optimized at B3LYP/6-31G(d) and CAM-B3LYP/6-31G(d) level respectively. The excitation energies were calculated via optimally turned LC-ωPBE (LC-ωPBE*) with 6-31G(d) basis set. The value of ω for each molecule is in the Table S6. In order to consider solvent effect, all the calculations were carrying out using the polarizable continuum model (PCM)[4], the solvent is toluene in the whole calculations. Anisotropy of the induced current density (AICD) calculations were carried out at the B3LYP/6-31+G(d) level. All of the above calculations were conducted using the Gaussian 16 package[5]. Hole-electron analysis[6] and NTOs were conducted utilizing Multiwfn.[7] The spin-orbital coupling between triplet and singlet states are calculated using Q-Chem[8] package using optimally turned LC-ωPBE08 functional with 6-31G(d) basis set. The oscillator strength between the triplet states, corresponding energy gap and singlet excited states energy are calculated using MS8-CASPT2 (8,8)/cc-pVDZ in OpenMolcas package[1] based on the T_1 geometry or S_1 geometry obtained by CAM-B3LYP/6-31G(d). The ISC rate from S_1 to T_1 is carried out in MOMAP package[9-11] using SOC calculated by Q-Chem (SOC value: 0.77 cm^{-1}) and excited state S_1 and T_1 frequency calculated by Gaussian 16 package.

2. The synthesis of compound TPA-DBPrz

2.1 The synthesis of (E)-3-(4-(diphenylamino)phenyl)-1-phenylprop-2-en-1-one (m3) 4-(N,N-diphenylamino)benzaldehyde (**m1**) 8.2 g (0.03 mol) and acetophenone 3.844 (**m2**) (0.033 mol) were mixed into a 100 ml round bottom flask with absolute alcohol (30 mL). The mixture was stirred at room temperature as well as PH=10 environment for 8 h and was filtered directly. After washing by alcohol and drying, **m3** was obtained as orange powder (8.2 g).

2.2 The synthesis of TPA-DBPrz Phenylhydrazine (**m4**) (10 ml) was added slowly to acetic acid (30 ml) and stirred for ten minutes at room temperature, then **m3** (0.022 mol) was added. The mixture was refluxed under nitrogen for 12 h. Then it was cooled to room temperature and poured into ice water. After filtering, the crude product was washed by alcohol and dried. The solid was purified by column chromatography (silica gel, dichloromethane:petroleum ether =3:1, volume ratio).

2.3 The ^{1}H NMR and ^{13}C NMR spectra:

The ^{1}H NMR and ^{13}C NMR spectra were recorded using a Bruker ADVANCE 400 NMR Spectrometer. All NMR spectra, if not otherwise specified, were measured at 25 ˚C and calibrated using the residual solvent signals. Elemental analysis was carried out on Flash EA 1112 Elemental Analyzer. The mass spectrum was acquired using a Bruker MOLDI-TOF instrument.

^{1}H NMR (400 MHz, THF-d8) δ 7.76 – 7.70 (m, 2H), 7.34 (dd, J = 8.3, 6.6 Hz, 2H), 7.30 – 7.25 (m, 1H), 7.19 (t, J = 8.0 Hz, 6H), 7.13 – 7.06 (m, 4H), 7.03 – 6.92 (m, 8H), 6.69 (tt, J = 6.5, 2.0 Hz, 1H), 5.29 (dd, J = 12.3, 7.0 Hz, 1H), 3.86 (dd, J = 17.1, 12.3 Hz, 1H), 3.13 (dd, J = 17.2, 7.0 Hz, 1H). MALDI: calculated 465.21999, found: 465.21994. Elemental analysis for $C_{33}H_{27}N_3$: C, 85.13%; H, 5.85%; N, 9.03%. Found: C, 85.12%; H, 5.83%; N, 9.02%.

3. Spectral characterization

3.1 UV-vis spectra The absorption spectra in solution were recorded by a Jasco V-570 spectrometer. Photoluminescence spectra of solution were recorded on a Jasco FP-6600 spectrophotometer. Absolute photoluminescence quantum yield was measured on a Jasco FP-6600 spectrophotometer equipped with an integrating sphere. Fluorescence decay measurements of the emitters were acquired in DCM solutions on a time-correlated single photon counting setup with excitation using a 390 nm laser. The degassed sample was bubbled under nitrogen for 20 minutes before measurement.

3.2 Femtosecond Transient Absorption Spectroscopy A femtosecond laser system (Pharos, Light Conversion) delivered laser pulses at 1030 nm (180 fs, 6 kHz), which were then divided into two components by using a 9:1 beam splitter. The major component was sent to an optical parametric amplifier (Orpheus, Light Conversion) to generate the pump pulses (400 nm, 6 kHz). The minor component was further attenuated and focused into a 3-mm sapphire plate to generate the probe pulses. Both the pump and probe pulses were guided into a Harppia spectrometer and time resolved spectral data were recorded. A short-pass filter was inserted into the probe beam to cut off the fundamental light of 1030 nm. The time delay between the pump and probe beams were regulated through a computer-controlled motorized translation stage in the probe beam. The temporal resolution between the pump and the probe pulses was determined to be ~200 fs (FWHM). The transmitted light was detected by a CMOS linear image sensor. The excitation pulsed energy was ~ 60 nJ/pulse as measured at the sample site. Analysis of

the kinetic traces derived from time-resolved spectra was performed using nonlinear least-square fitting to a general sum-of-exponentials function after deconvolution of instrument response function (IRF). All the spectroscopic measurements were carried out at room temperature.

3.3 Nanosecond-to-microsecond transient absorption Experiments were performed using a commercial nanosecond laser flash photolysis spectrometer (LP980-KS, Edinburgh Instruments Ltd., Livingston, UK) at ambient temperature. The pump laser pulse was obtained from Optical Parametric Oscillator (PrimoScan ULD400, Spectra-Physics) at 532 nm, with the FWHM of no more than 10 ns. The probe light was provided by a 150 W Pulsed xenon arc lamp. Sample solution in 1×1cm optical quartz cuvette was excited by the pump laser, afterwards the probe light from the xenon lamp passed through the sample in a right-angle configuration. The transmission probe light was measured either by a single PMT detector (Hamamatsu R928), using a Tektronix Model MDO3052 (100 MHz, 1.25 GSs-1) digital oscilloscope, at a specified wavelength for kinetic analysis or by a ICCD camera (DH320T, Andor) for spectral analysis. All the samples were bubbled under nitrogen for 20 minutes before measurement.

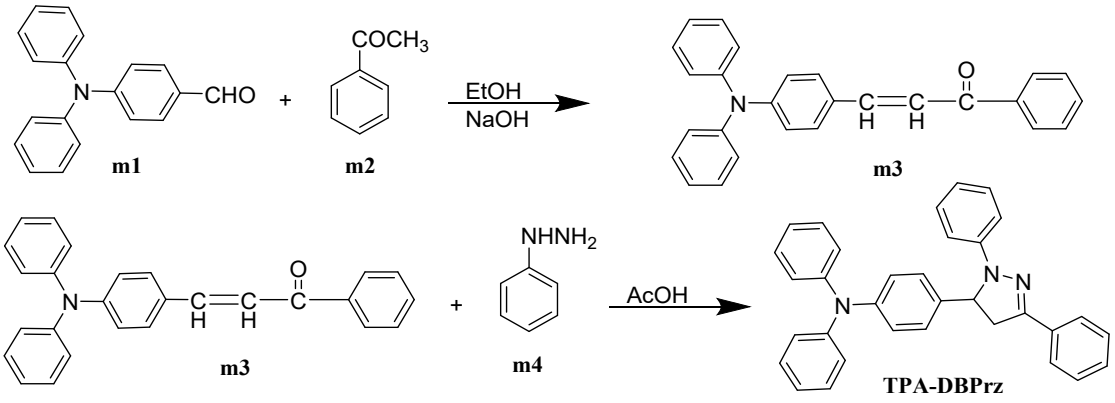

Scheme S1. Synthetic route to compound TPA-DBPrz**.**

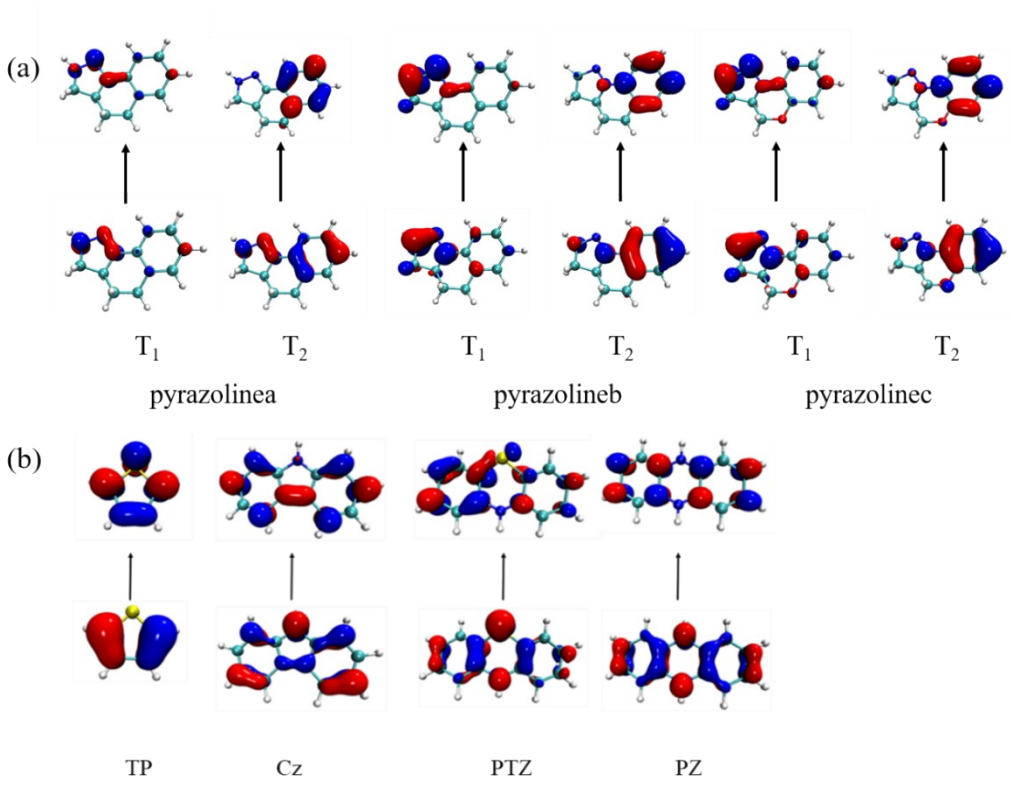

Figure S1. (a) NTOs of pyrazolinea, pyrazolineb and pyrazolinc at T_1 and T_2 states respectively at the level of TDA-LC-ωPBE*/6-31G(d). (b) The electronic charge of involved molecular orbitals in T_1 state for TP, Cz, PTZ and PZ.

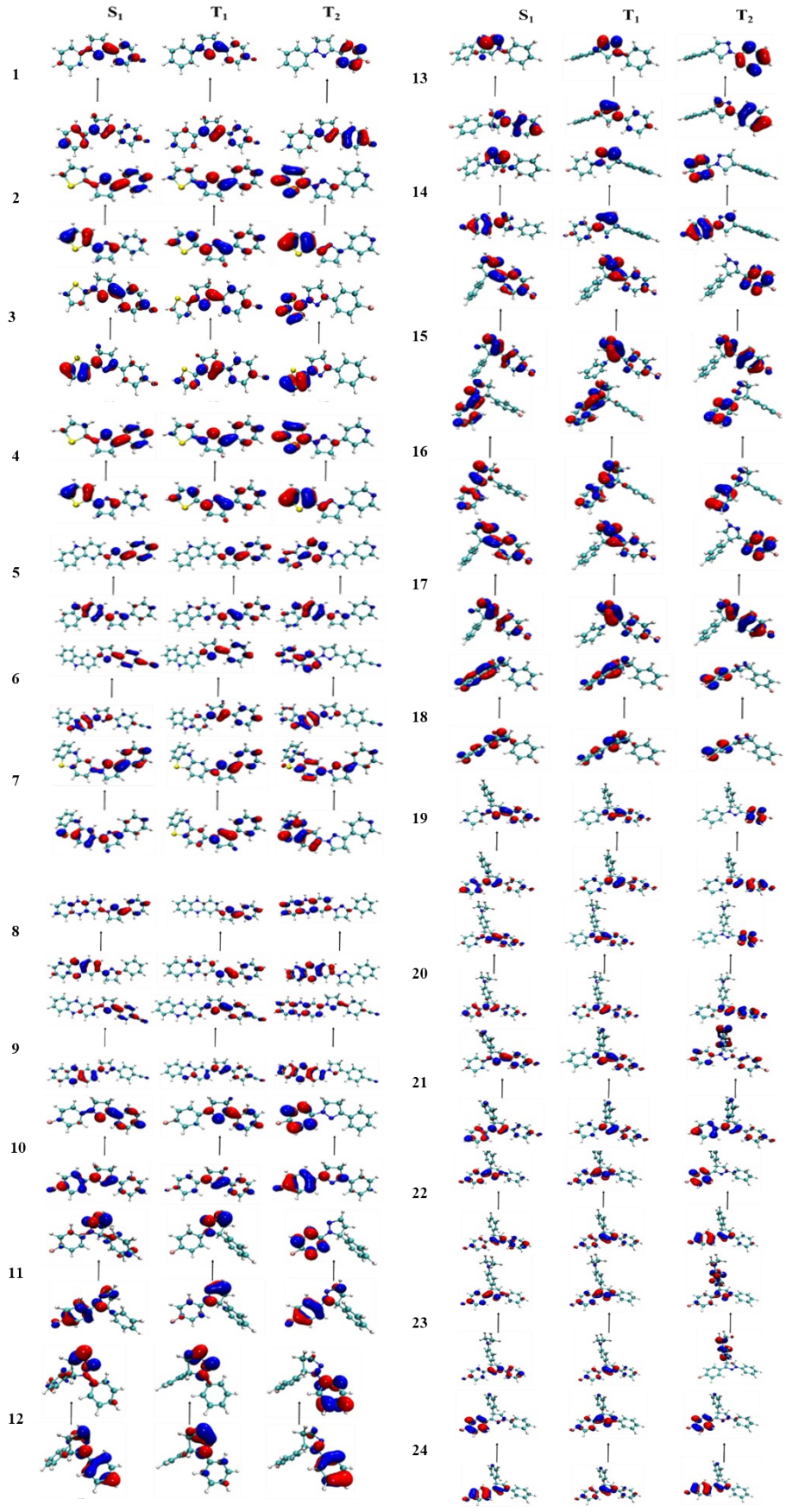

Figure S2. NTOs of the S_1, T_1 and T_2 states at the corresponding S_1-, T_1-, T_1-geometry respectively for compounds **1-24**.

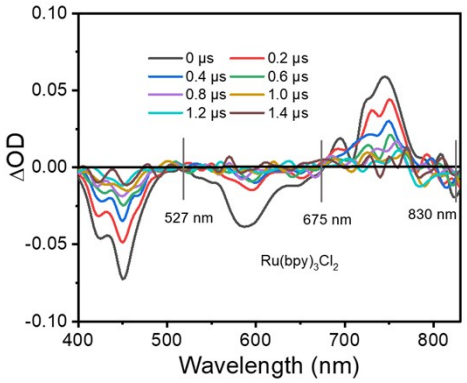

Figure S3. ns-TA measurement of $Ru(bpy)_3Cl_2$ (20 mM) at different time delay.

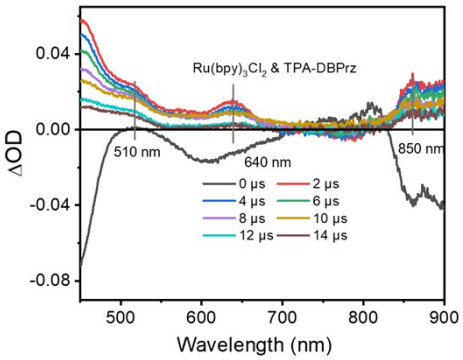

Figure S4. ns-TA measurement of $Ru(bpy)_3Cl_2$ (20 uM) &TPA-DBPrz (1 mM) at different time delay.

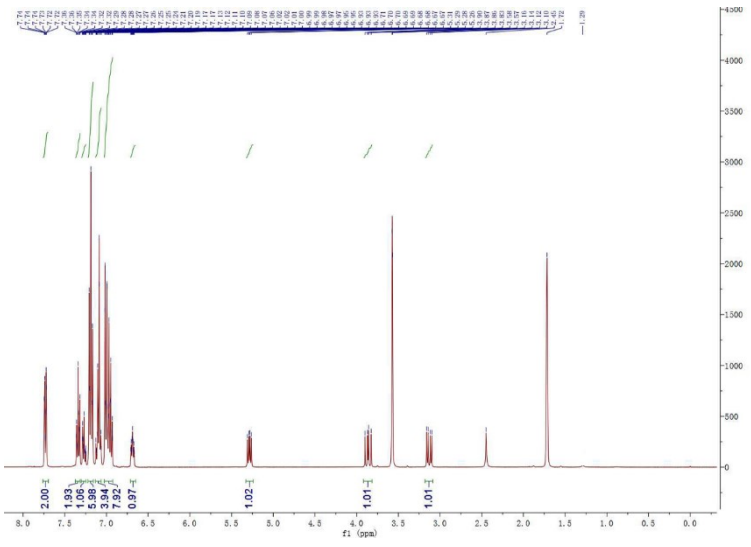

Figure S5. ^1H NMR (400 MHz, THF-d8) of compound TPA-DBPrz.

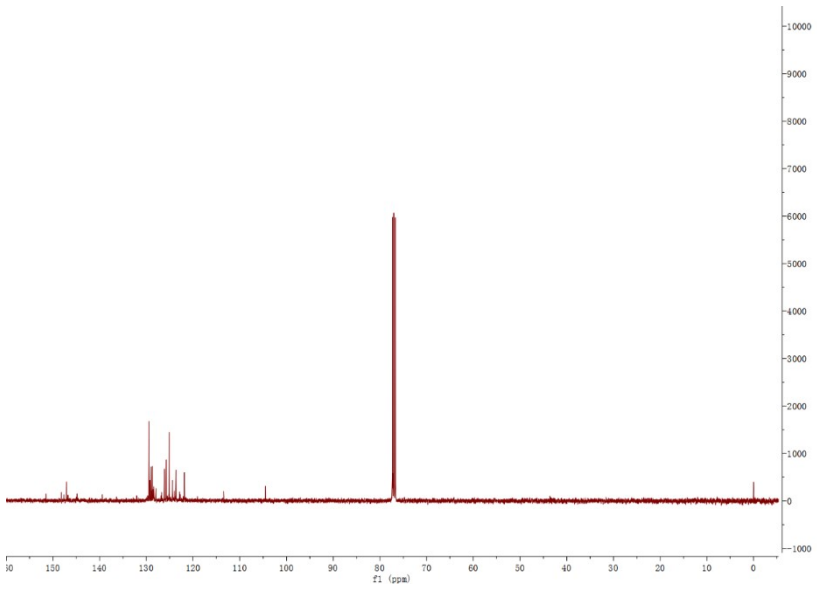

Figure S6. ^{13}C NMR (100 MHz, THF-d8) of compound TPA-DBPrz.

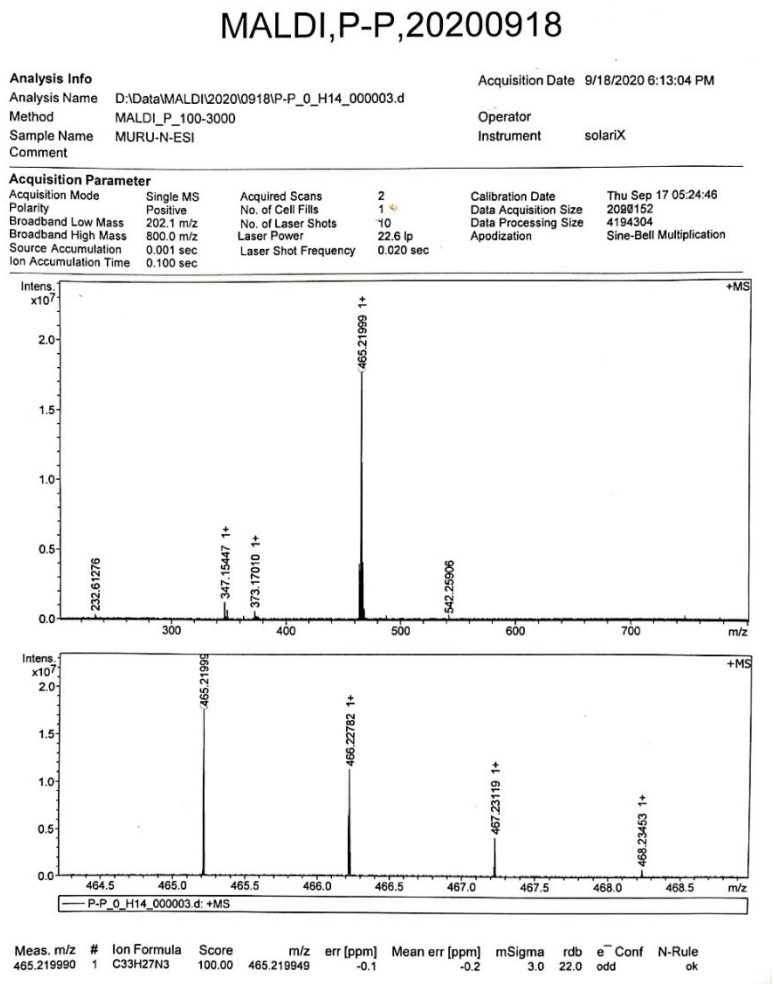

Figure S7. High resolution mass spectrometry of TPA-DBPrz.

Table S1. The transitions of S_1, T_1 and T_2 states for the five-membered rings at T_1-geometry at the level of MS4-CASPT2/cc-PVTZ and TDA-LC-ωPBE*/6-31G(d) with optimally-tuned ω* values (Unit: $Bohr^{-1}$) .

Compound	MS4-CASPT2/cc-PVTZ			LC-ωPBE*/6-31G(d)			ω*
	T_1	T_2	S_1	T_1	T_2	S_1	
cyclopentene	H -> L 96%	H-4 -> L 94%	H -> L 79% H-2->L 10%	H -> L 98%	H-2 -> L 46% H-4 -> L 38%	H -> L 90%	0.2762
3-pyrroline	H -> L 88%	H-1 -> L 87%	H -> L+1 32% H -1-> L+1 42%	H -> L 89%	H-1 -> L 90%	H-1 -> L 78% H -> L 21%	0.2863
pyrazoline	H -> L 90%	H-1 -> L 39% H-3 -> L 51%	H -> L 89%	H -> L 96%	H-1 -> L 98%	H -> L 90%	0.3422
pyrazole	H -> L 38% H-1 -> L 48%	H -> L 29% H-1 -> L 34%	H-2 -> L 15% H-1 -> L 28%	H -> L 97%	H-1 -> L 95%	H-2 -> L 76% H-1 -> L 17%	0.3400
imidazole	H -> L+1 79%	H -> L+4 46% H-1 -> L+1 33%	H -> L+1 48% H-1 -> L+1 14%	H -> L 98%	H-1 -> L 92%	H -> L 97%	0.3035
pyrrole	H -> L+1 87%	H -> L+3 35% H-1 -> L+1 47%	H -> L+2 30% H-1 -> L+1 38%	H -> L 98%	H-1 -> L 54% H -> L 46%	H -> L 98%	0.3020

Table S2. Vertical excitation energies (Unit: eV) of the five-membered rings at T_1-geometry at the level of TDA-LC-ωPBE*/6-31G(d).

Compound	$E(T_1)$	$E(T_2)$	$E(S_1)$	$2E(T_1)$	$\Delta E(T_1T_2)$
cyclopentene	0.41	5.32	3.88	0.82	4.91
3-pyrroline	0.74	3.46	3.49	1.48	2.72
pyrazoline	1.43	4.56	4.48	2.86	3.13
pyrazole	2.73	4.50	5.64	5.46	1.77
imidazole	3.02	5.16	5.93	6.04	2.14
pyrrole	2.94	5.18	5.96	5.88	2.24

Table S3. Optimally-tuned ω* values for the LC-ωPBE functional and vertical excitation energies at T_1 geometry of compound pyrazoline-a to pyrazoline-c at the level of TDA-LC-ωPBE*/6-31G(d) (Unit: eV).

Compound	ω*	$E(T_1)$	$E(T_2)$	$E(S_1)$
pyrazoline-a	0.2303	1.34	3.94	3.86
pyrazoline-b	0.2386	1.70	3.82	4.03
pyrazoline-c	0.2375	1.66	3.84	3.90

Table S4. E_{HOMO} and E_{LUMO} of the donors and acceptors investigated in this work calculated at the level of B3LYP/6-31G* (Unit: eV).

Compound	E_{HOMO}	E_{LUMO}
TP	-6.33	-0.21
Cz	-5.44	-0.64
PTZ	-4.76	-0.44
PZ	-4.14	-0.88
FB	-6.62	-0.24
Py	-6.78	-0.61
BN	-7.26	-1.41

Table S5. Significantly changed bonds (Unit: Å) of the investigated compounds in Scheme 1 (L_n^A means bond L_n at A geometry)

Compound	$L_1^{S_0}$	$L_1^{S_1}$	$L_1^{T_1}$	$L_2^{S_0}$	$L_2^{S_1}$	$L_2^{T_1}$	$L_3^{S_0}$	$L_3^{S_1}$	$L_3^{T_1}$
1	1.295	1.365	1.431	1.461	1.406	1.389	1.389	1.36	1.391
2	1.296	1.360	1.428	1.462	1.412	1.391	1.382	1.332	1.367
3	1.298	1.349	1.416	1.458	1.415	1.393	1.38	1.327	1.362
4	1.300	1.347	1.414	1.455	1.412	1.392	1.398	1.348	1.389
5	1.301	1.341	1.403	1.454	1.412	1.384	1.399	1.352	1.388
6	1.353	1.348	1.420	1.458	1.412	1.392	1.391	1.347	1.387
7	1.299	1.341	1.409	1.456	1.410	1.383	1.392	1.35	1.387
8	1.297	1.334	1.418	1.461	1.423	1.391	1.393	1.345	1.382
9	1.301	1.327	1.382	1.454	1.417	1.391	1.396	1.341	1.364
10	1.296	1.364	1.431	1.391	1.359	1.390	1.462	1.407	1.389
11	1.293	1.380	1.447	1.521	1.512	1.516	1.467	1.403	1.386
12	1.293	1.380	1.446	1.466	1.403	1.386	1.521	1.512	1.516
13	1.293	1.382	1.440	1.471	1.403	1.390	1.517	1.517	1.521
14	1.294	1.382	1.440	1.517	1.517	1.521	1.471	1.403	1.390
15	1.283	1.384	1.447	1.398	1.362	1.390	1.518	1.514	1.513

16	1.283	1.385	1.447	1.518	1.513	1.512	1.397	1.365	1.391
17	1.282	1.362	1.453	1.520	1.506	1.516	1.402	1.350	1.394
18	1.282	1.360	1.452	1.404	1.347	1.393	1.520	1.506	1.516
19	1.296	1.366	1.430	1.464	1.409	1.391	1.393	1.361	1.391
20	1.296	1.366	1.431	1.465	1.408	1.390	1.392	1.361	1.391
21	1.296	1.365	1.430	1.464	1.411	1.391	1.395	1.362	1.392
22	1.293	1.367	1.431	1.463	1.408	1.390	1.398	1.362	1.394
23	1.294	1.366	1.431	1.462	1.408	1.390	1.396	1.362	1.393
24	1.293	1.367	1.432	1.400	1.410	1.390	1.463	1.364	1.395
TPA-DBPrz	1.294	1.346	1.431	1.463	1.423	1.390	1.397	1.344	1.394

Table S6. Optimally-tuned ω* values for the LC-ωPBE functional with 6-31G(d) basis sets, corresponding oscillator strengths (*f*) of S_1 state and vertical transition energies at S_1-geometry (Unit: eV).

Compound	ω*	f	$E(T_1)$	$E(S_1)$	$E(T_2)$
1	0.2032	1.067	1.86	3.27	3.66
2	0.2076	0.864	1.77	3.00	3.17
3	0.2084	0.789	1.70	2.87	3.20
4	0.1854	1.207	1.76	2.94	2.92
5	0.1904	1.460	1.67	2.78	2.93
6	0.1879	1.035	1.83	2.96	3.11
7	0.1829	1.248	1.73	2.80	3.03
8	0.1872	0.634	1.80	2.63	2.43
9	0.1871	0.822	1.53	2.30	2.42
10	0.2047	1.041	1.86	3.24	3.43
11	0.2447	0.270	2.30	3.67	3.48
12	0.2385	0.279	2.31	3.67	3.81
13	0.1941	0.098	1.87	2.66	3.63
14	0.2216	0.109	1.86	2.65	3.63
15	0.2429	0.675	1.82	3.94	3.83
16	0.2417	0.698	1.82	3.92	3.96
17	0.2398	0.658	1.82	3.83	3.98
18	0.2411	0.682	1.82	3.80	3.82
19	0.2007	0.917	1.83	3.20	3.65
20	0.1960	0.957	1.85	3.21	3.64
21	0.2010	0.798	1.81	3.15	3.65
22	0.2023	0.943	1.82	3.19	3.65
23	0.1977	0.976	1.82	3.18	3.65
24	0.2036	0.838	1.82	3.15	3.65
TPA-DBPrz	0.1802	0.894	1.80	3.12	3.32

Table S7. Calculated triplet gaps and corresponding oscillator strength using MS8-CASPT2 (8,8)/cc-pVDZ.

Transition	Δ*E*	*f*
T_1->T_2	1.68	0.00672
T_1->T_3	1.83	0.00011
T_1->T_4	2.19	0.00224
T_1->T_5	2.36	0.00003
T_1->T_6	2.94	0.00000

References

1 F. Aquilante, J. Autschbach, R. K. Carlson, L. F. Chibotaru, M. G. Delcey, L. De Vico, I. Fdez Galvan, N. Ferre, L. M. Frutos, L. Gagliardi, M. Garavelli, A. Giussani, C. E. Hoyer, G. Li Manni, H. Lischka, D. Ma, P. A. Malmqvist, T. Muller, A. Nenov, M. Olivucci, T. B. Pedersen, D. Peng, F. Plasser, B. Pritchard, M. Reiher, I. Rivalta, I. Schapiro, J. Segarra-Marti, M. Stenrup, D. G. Truhlar, L. Ungur, A. Valentini, S. Vancoillie, V. Veryazov, V. P. Vysotskiy, O. Weingart, F. Zapata, R. Lindh, *J. Comput. Chem.*, **2016**, *37*, 506-541.

2 M. J. Peach, M. J. Williamson, D. J. Tozer, *J. Chem. Theory Comput.*, **2011**, *7*, 3578-3585.

3 aP. K. Samanta, D. Kim, V. Coropceanu, J. L. Bredas, *J. Am. Chem. Soc.* **2017**, *139*, 4042-4051; bH. Sun, C. Zhong, J. L. Bredas, *J Chem Theory Comput.*, **2015**, *11*, 3851-3858.

4 G. Scalmani, M. J. Frisch, *J. Chem. Phys.*, **2010**, *132*, 114110.

5 M. J. Frisch, G. W. Trucks, H. B. Schlegel, G. E. Scuseria, M. A. Robb, J. R. Cheeseman, G. Scalmani, V. Barone, G. A. Petersson, H. Nakatsuji, X. Li, M. Caricato, A. V. Marenich, J. Bloino, B. G. Janesko, R. Gomperts, B. Mennucci, H. P. Hratchian, J. V. Ortiz, A. F. Izmaylov, J. L. Sonnenberg, Williams, F. Ding, F. Lipparini, F. Egidi, J. Goings, B. Peng, A. Petrone, T. Henderson, D. Ranasinghe, V. G. Zakrzewski, J. Gao, N. Rega, G. Zheng, W. Liang, M. Hada, M. Ehara, K. Toyota, R. Fukuda, J. Hasegawa, M. Ishida, T. Nakajima, Y. Honda, O. Kitao, H. Nakai, T. Vreven, K. Throssell, J. A. Montgomery Jr., J. E. Peralta, F. Ogliaro, M. J. Bearpark, J. J. Heyd, E. N. Brothers, K. N. Kudin, V. N. Staroverov, T. A. Keith, R. Kobayashi, J. Normand, K. Raghavachari, A. P. Rendell, J. C. Burant, S. S. Iyengar, J. Tomasi, M. Cossi, J. M. Millam, M. Klene, C. Adamo, R. Cammi, J. W. Ochterski, R. L. Martin, K. Morokuma, O. Farkas, J. B. Foresman, D. J. Fox, Wallingford, CT, **2016**.

6 Z. Liu, T. Lu, Q. Chen, *Carbon*, **2020**, *165*, 461-467.

7 a) T. Lu, F. Chen, *J. Comput. Chem.*, **2012**, *33*, 580-592; b) E. Menard, V. Podzorov, S. H. Hur, A. Gaur, M. E. Gershenson, J. A. Rogers, *Adv. Mater.*, **2004**, *16*, 2097-2101.

8 Y. Shao, Z. Gan, E. Epifanovsky, A. T. B. Gilbert, M. Wormit, J. Kussmann, A. W. Lange, A. Behn, J. Deng, X. Feng, D. Ghosh, M. Goldey, P. R. Horn, L. D. Jacobson, I. Kaliman, R. Z. Khaliullin, T. Kuś, A. Landau, J. Liu, E. I. Proynov, Y. M. Rhee, R. M. Richard, M. A. Rohrdanz, R. P. Steele, E. J. Sundstrom, H. L. Woodcock, P. M. Zimmerman, D. Zuev, B. Albrecht, E. Alguire, B. Austin, G. J. O. Beran, Y. A. Bernard, E. Berquist, K. Brandhorst, K. B. Bravaya, S. T. Brown, D. Casanova, C.-M. Chang, Y. Chen, S. H. Chien, K. D. Closser, D. L. Crittenden, M. Diedenhofen, R. A. DiStasio, H. Do, A. D. Dutoi, R. G. Edgar, S. Fatehi, L. Fusti-Molnar, A. Ghysels, A. Golubeva-Zadorozhnaya, J. Gomes, M. W. D. Hanson-Heine, P. H. P. Harbach, A. W. Hauser, E. G. Hohenstein, Z. C. Holden, T.-C. Jagau, H. Ji, B. Kaduk, K. Khistyaev, J. Kim, J. Kim, R. A. King, P. Klunzinger, D. Kosenkov, T. Kowalczyk, C. M. Krauter, K. U. Lao, A. D. Laurent, K. V. Lawler, S. V. Levchenko, C. Y. Lin, F. Liu, E. Livshits, R. C. Lochan, A. Luenser, P. Manohar, S. F. Manzer, S.-P. Mao, N. Mardirossian, A. V. Marenich, S. A. Maurer, N. J. Mayhall, E. Neuscamman, C. M. Oana, R. Olivares-Amaya, D. P. O'Neill, J. A. Parkhill, T. M. Perrine, R. Peverati, A. Prociuk, D. R. Rehn, E. Rosta, N. J. Russ, S. M. Sharada, S. Sharma, D. W. Small, A. Sodt, et al., *Mol. Phys.*, **2014**, *113*, 184-215.

9 Y. Niu, W. Li, Q. Peng, H. Geng, Y. Yi, L. Wang, G. Nan, D. Wang and Z. Shuai, *Mol. Phys.*, **2018**, *116*, 1078-1090.

10 Q. Peng, Y. Yi, Z. Shuai and J. Shao, *J. Am. Chem. Soc.*, **2007**, *129*, 9333-9339.

11 Q. Peng, Y. Niu, Q. Shi, X. Gao and Z. Shuai, *J. Chem. Theory Comput.*, **2013**, *9*, 1132-1143.